EPJ manuscript No.
(will be inserted by the editor)

The JLab Upgrade - Studies of the Nucleon with CLAS12.

Selected topics

Volker D. Burkert

Jefferson Lab, Newport News, Virginia, USA

February 2, 2008

Abstract. An overview is presented on the program to study the nucleon structure at the 12 GeV JLab upgrade using the CLAS12 detector. The focus is on deeply virtual exclusive processes to access the generalized parton distributions, semi-inclusive processes to study transverse momentum dependent distribution functions and inclusive spin structure functions, and resonance transition form factors at high Q^2 and with high precision.

PACS. 1 1.55.Fv, 13.60.Le, 13.40.Gp, 14.20.Gk

1 Introduction

The challenge of understanding nucleon electromagnetic structure still continues after more than five decades of experimental scrutiny. From the initial measurements of elastic form factors to the accurate determination of parton distributions through deep inelastic scattering (DIS), the experiments have increased in statistical and systematic accuracy. Only recently it was realized that the parton distribution functions represent special cases of a more general, much more powerful, way to characterize the structure of the nucleon, the generalized parton distributions (GPDs) [1,2,3,4]. The GPDs are the Wigner quantum phase space distribution of quarks in the nucleon – functions describing the simultaneous distribution of particles with respect to both position and momentum in a quantum-mechanical system, representing the closest analogue to a classical phase space density allowed by the uncertainty principle. In addition to the information about the spatial density (form factors) and momentum density (parton distribution), these functions reveal the correlation of the spatial and momentum distributions, *i.e.* how the spatial shape of the nucleon changes when probing quarks and gluons of different wavelengths.

The concept of GPDs has led to completely new methods of "spatial imaging" of the nucleon, either in the form of two-dimensional tomographic images (analogous to CT scans in medical imaging), or in the form of genuine three-dimensional images (Wigner distributions). GPDs also allow us to quantify how the orbital motion of quarks in the nucleon contributes to the nucleon spin – a question of crucial importance for our understanding of the "mechanics" underlying nucleon structure. The spatial view of the nucleon enabled by the GPDs provides us with new ways to test dynamical models of nucleon structure.

The mapping of the nucleon GPDs, and a detailed understanding of the spatial quark and gluon structure of the nucleon, have been widely recognized as the key objectives of nuclear physics of the next decade. This requires a comprehensive program, combining results of measurements of a variety of processes in electron–nucleon scattering with structural information obtained from theoretical studies, as well as with expected results from future lattice QCD simulations.

While GPDs, and also the recently introduced transverse momentum dependent distribution functions (TMDs), open up new avenues of research, the traditional means of studying the nucleon structure through electromagnetic elastic and transition form factors, and through flavor- and spin-dependent parton distributions must also be employed with high precision to extract physics on the nucleon structure in the transition from the regime of quark confinement to the domain of asymptotic freedom. These avenues of research can be explored using the 12 GeV cw beam of the JLab upgrade with much higher precision than has been achieved ever before, and can help reveal some of the remaining secrets of QCD, such as the origin of confinement. Also, the high luminosity available will allow to explore the regime of extreme quark momentum, where a single quark carries 80% or more of the proton's total momentum. To meet the requirements of high statistics measurements of relatively rare exclusive processes the equipment will be upgraded and include the CLAS12 large acceptance spectrometer. The main new features of CLAS12 over the current CLAS detector include a high operational luminosity of $10^{35}\mathrm{cm}^{-2}\mathrm{sec}^{-1}$, an order of magnitude increase over CLAS [5]. Improved particle identification and event reconstruction will be achieved with additional threshold gas Cerenkov counter, improved timing resolution of the forward time-of-flight system, and a

new central detector that uses a high-field solenoid magnet for particle tracking and the operation of a polarized targets. With these upgrades CLAS12 will be the workhorse for exclusive and semi-inclusive electroproduction experiments in the deep inelastic kinematics.

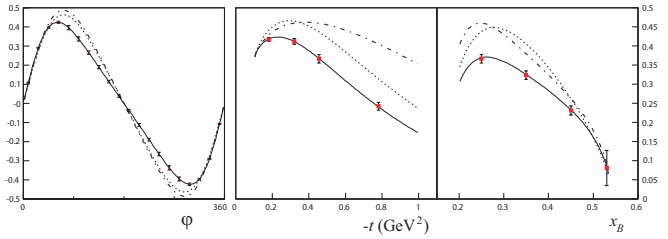

Fig. 1. The beam spin asymmetry showing the DVCS-BH interference for 11 GeV beam energy [7]. Left panel: $x = 0.2$, $Q^2 = 3.3\text{GeV}^2$, $-t = 0.45\text{GeV}^2$. Middle and right panels: $\phi = 90^\circ$, other parameters same as in left panel. Many other bins will be measured simultaneously. The curves represent various parameterizations within the VGG model [6]. Projected uncertainties are statistical.

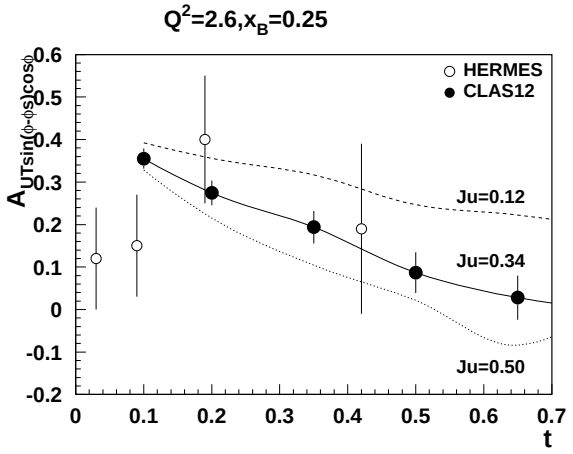

Fig. 2. Projected transverse target asymmetry A_{UT} for DVCS production off protons at 11 GeV beam energy.

2 Generalized Parton Distributions and DVCS

It is well recognized [1,8,9,10] that exclusive processes can be used to probe the GPDs and construct 2-dimensional and 3-dimensional images of the quark content of the nucleon. Deeply virtual Compton scattering and deeply virtual meson production are identified as the processes most suitable to map out at the twist-2 vector GPDs H, E and the axial GPDs $\tilde{H}$, $\tilde{E}$ in x, ξ, t, where x is the momentum fraction of the struck quark, ξ the longitudinal momentum transfer to the quark, and t the transverse momentum transfer to the nucleon. Having access to a 3-dimensional image of the nucleon (two dimensions in transverse space, one dimension in longitudinal momentum) opens up completely new insights into the complex structure of the nucleon. In addition, GPDs carry information of more global nature. For example, the nucleon matrix element of the energy-momentum tensor contains 3 form factors that encode information on the angular momentum distribution $J^q(t)$ of the quarks with flavor q in transverse space, their mass-energy distribution $M_2^q(t)$, and their pressure and force distribution $d_1^q(t)$. How can we access these form factors? The only known process to directly measure them is elastic graviton scattering off the nucleon. However, today we know that these form factors also appear as moments of the vector GPDs [11], thus offering prospects of accessing these quantities through detailed mapping of GPDs. The quark angular momentum in the nucleon is given by

$$J^q(t) = \int_{-1}^{+1} dx x[H^q(x,\xi,t) + E^q(x,\xi,t)] \ ,$$

and the mass-energy and pressure distribution

$$M_2^q(t) + 4/5 d_1^q(t)\xi^2 = \int_{-1}^{+1} dx x H^q(x,\xi,t) \ .$$

The mass-energy and force-pressure distribution of the quarks are given by the second moment of GPD H, and their relative contribution is controlled by ξ. A separation of $M_2^q(t)$ and $d_1^q(t)$ requires measurement of these moments in a large range of ξ. The beam helicity-dependent cross section asymmetry is given in leading twist as

$$A_{LU} \approx \sin\phi[F_1(t)H + \xi(F_1+F_2)\tilde{H}]d\phi \ ,$$

where ϕ is the azimuthal angle between the electron scattering plane and the hadronic plane. The kinematically suppressed term with GPD E is omitted. The asymmetry is mostly sensitive to the GPD $H(x=\xi,\xi,t)$. In a wide kinematics [12,13] the beam asymmetry A_{LU} was measured at Jefferson Lab at modestly high Q^2, ξ, and t, and in a more limited kinematics [14] the cross section difference $\Delta\sigma_{LU}$ was measured with high statistics. Moreover, a first measurement of the target asymmetry $A_{UL} = \Delta\sigma_{UL}/2\sigma$ was carried out [15], where

$$A_{UL} \approx \sin\phi[F_1\tilde{H} + \xi(F_1+F_2)H] \ .$$

The combination of A_{LU} and A_{UL} allows to separate GPD $H(x=\xi,\xi,t)$ and $\tilde{H}(x=\xi,\xi,t)$. Using a transversely polarized target the asymmetry

$$A_{UT} \approx \cos\phi\sin(\phi-\phi_s)[t/4M^2(F_2H - F_1E)]$$

can be measured, where ϕ_s is the azimuthal angle of the target polarization vector relative to the electron scattering plane. A_{UT} depends in leading order on GPD E.

The 12 GeV upgrade offers much improved possibilities to access GPDs. Figure 1 shows the expected statistical precision of the beam DVCS asymmetry for some

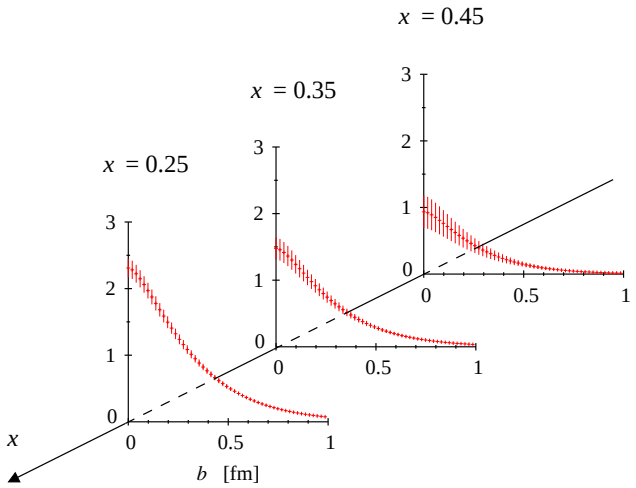

Fig. 3. The u-quark distribution in transverse space as extracted from projected DVCS data with CLAS12.

sample kinematics. Using a polarized target one can also measure the target spin asymmetries with high precision. Figure 2 shows the expected statistical accuracy for one kinematics bin. A measurement of all 3 asymmetries will allow a separate determination of GPDs H, $\tilde{H}$ and E at the above specified kinematics. Through a Fourier transformation the t-dependence of GPD H can be used to determine the $u-$quark distribution in transverse impact parameter space. Figure 3 shows projected results.

Deeply virtual meson production will play an important role in disentangling the flavor- and spin-dependence of GPDs. For exclusive mesons only the longitudinal photon coupling in $\gamma^* p \rightarrow Nm$ allows direct access to GPDs through the handbag mechanism and must be isolated from the transverse coupling. Also, the dominance of the handbag mechanism must first be established at the upgrade energy.

3 Transverse momentum dependent parton distributions and SIDIS

Semi-inclusive deep inelastic scattering (SIDIS) studies, when a hadron is detected in coincidence with the scattered lepton that allows so-called "flavor tagging", provide more direct access to contributions from various quarks. In addition, they give access to the transverse momentum distributions of quarks, not accessible in inclusive scattering. Azimuthal distributions of final state particles in semi-inclusive deep inelastic scattering provide access to the orbital motion of quarks and play an important role in the study of TMDs of quarks in the nucleon.

TMD distributions (see Table 1) describe transitions of a nucleon with one polarization in the initial state to a quark with another polarization in the final state. The diagonal elements of the table are the momentum, longitudinal and transverse spin distributions of partons, and represent well-known parton distribution functions related

N/q	U	L	T
U	$\mathbf{f_1}$		$h_1^\perp$
L		$\mathbf{g_1}$	$h_{1L}^\perp$
T	$f_{1T}^\perp$	g_{1T}	$\mathbf{h_1}$ $h_{1T}^\perp$

Table 1. Leading-twist transverse momentum-dependent distribution functions. U, L, and T stand for transitions of unpolarized, longitudinally polarized, and transversely polarized nucleons (rows) to corresponding quarks (columns).

to the square of the leading-twist, light-cone wave functions. Off-diagonal elements require non-zero orbital angular momentum and are related to the wave function overlap of L=0 and L=1 Fock states of the nucleon [16]. The chiral-even distributions $f_{1T}^\perp$ and g_{1T} are the imaginary parts of the corresponding interference terms, and the chiral-odd $h_1^\perp$ and h_{1L} are the real parts. The TMDs $f_{1T}^\perp$ and $h_1^\perp$, which are related to the imaginary part of the interference of wave functions for different orbital momentum states and are known as the Sivers and Boer-Mulders functions, and describe unpolarized quarks in the transversely polarized nucleon and transversely polarized quarks in the unpolarized nucleon respectively. The most simple mechanism that can lead to a Boer-Mulders function is a correlation between the spin of the quarks and their orbital angular momentum. In combination with a final state interaction that is on average attractive, already a measurement of the sign of the Boer-Mulders function, would thus reveal the correlation between orbital angular momentum and spin of the quarks.

Similar to GPDs, TMD studies will benefit from the higher energy and high luminosity at 12 GeV. A comprehensive program is in preparation with CLAS12 to study the new structure functions. Examples of expected uncertainties [17] for the Boer-Mulders asymmetry $A_{UU}^{cos2\phi}$ are presented in Fig. 4. Projections of the Mulders function h_{1L}^u for $u-$quarks from π^+ asymmetries A_{UL} with CLAS12 are shown in Fig. 5, and compared with preliminary results from the CLAS EG1 data set at 5.75 GeV beam energy.

4 Inclusive structure functions and moments

Polarized and unpolarized structure functions of the nucleon offer a unique window on the internal quark structure of stable baryons. The study of these structure functions provides insight into the two defining features of QCD — asymptotic freedom at small distances, and confinement and non-perturbative effects at large distance scales. After more than three decades of measurements at many accelerator facilities worldwide, a truly impressive amount of data has been collected, covering several orders of magnitude in both kinematic variables x and Q^2. However, there are still important regions of the kinematic phase space where data are scarce and have large errors and where significant improvements are possible through experiments at Jefferson Lab with an 11 GeV electron beam.

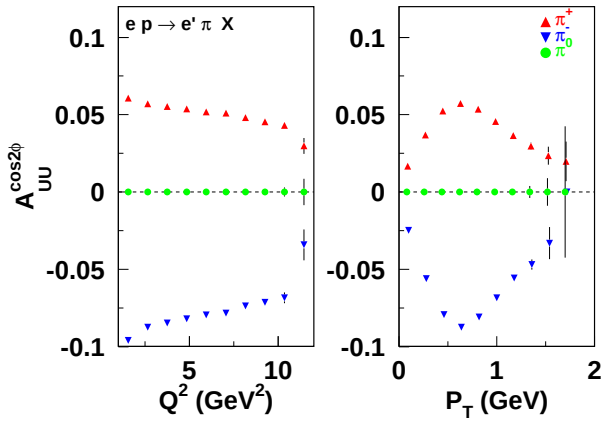

Fig. 4. The $\cos 2\phi$ moment (Boer-Mulders asymmetry) for pions as a function of Q^2 and P_T for $Q^2 > 2$ GeV^2 (right) with CLAS12 at 11 GeV from 2000 hours of running. Values are calculated assuming $H_1^{\perp u\to\pi^+} = -H_1^{\perp u\to\pi^-}$. Only statistical uncertainties are shown.

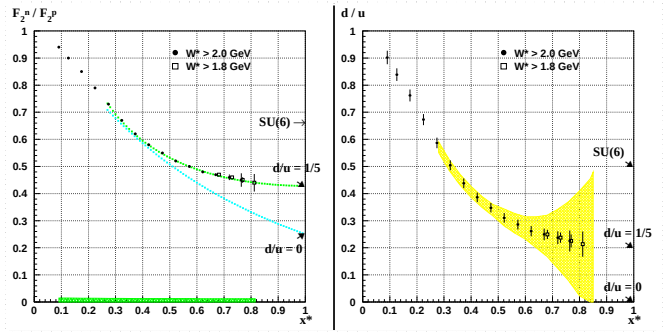

Fig. 6. Projected data for the ratio F_2^n/F_2^p (left) and d/u (right) for 11 GeV beam energy [19]. The error bars in the right panel contain both statistical and systematic uncertainties. The yellow area shows the uncertainty of current data due to poorly known nuclear corrections.

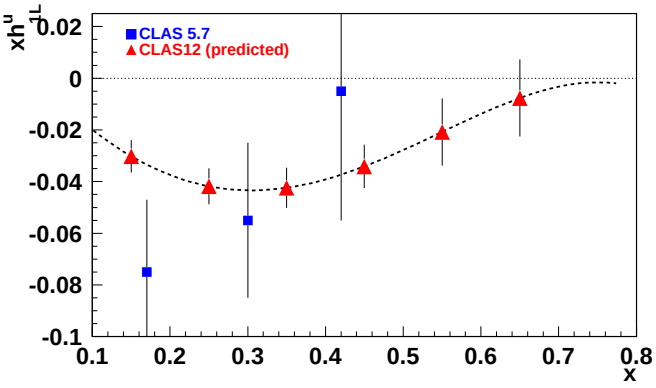

Fig. 5. Projected data from CLAS12 for the chiral odd function h_{1L}^u for u-quarks.

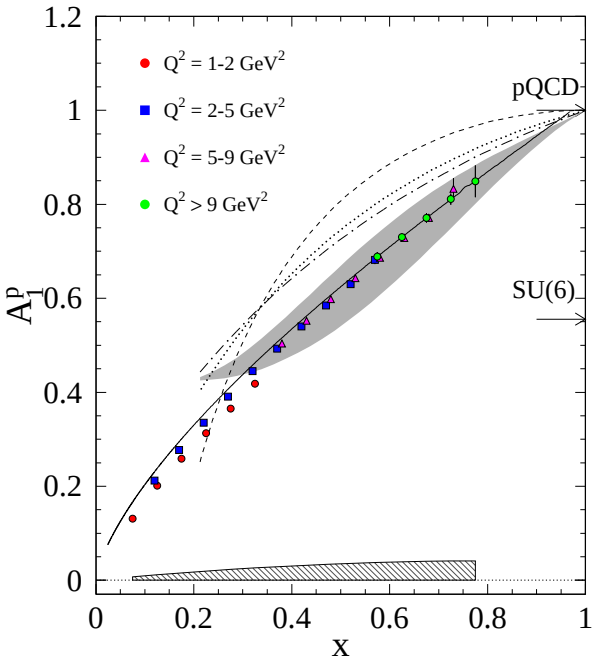

Fig. 7. Anticipated results on A_1^p.The four different symbols represent four different Q^2 ranges. The statistical uncertainty is given by the error bars while the systematic uncertainty is given by the shaded band.

One of the most interesting open questions is the behavior of the structure functions in the extreme kinematic limit $x \to 1$. In this region effects from the virtual sea of quark-antiquark pairs are suppressed, making this region simpler to model. This is also the region where pQCD can make absolute predictions. However, the large x domain is hard to reach because cross sections are kinematically suppressed, the parton distributions are small and final states interactions (partonic or hadronic) are large. First steps into the large x domain became possible with 5-6 GeV [18,20,21,22]. The interest triggered by these first results and the clear necessity to extend the program to larger x provided one of the cornerstone of the JLab 12 GeV upgrade physics program.

4.1 Valence quark structure and flavor dependence at large x.

The unpolarized structure function $F_2^p(x)$ has been mapped out in a large range of x leading to precise knowledge of the quark distribution $u(x)$. The corresponding structure function $F_2^n(x)$ is, however, well measured only for $x < 0.5$ as nuclear corrections, when using deuterium as a target, become large at large x and are not well represented by Fermi motion. At JLab a new technique tested recently with CLAS has been shown to be very effective in reducing the nuclear corrections. The BONUS experiment [18] has recently taken data using a novel radial TPC with GEM

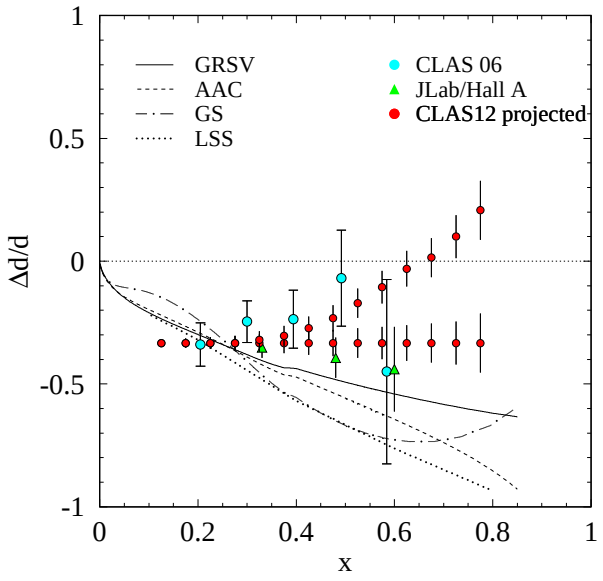

Fig. 8. Expected results for $(\Delta d + \Delta\bar{d})/(d + \bar{d})$. The central values of the data are following two arbitrary curves to demonstrate how the two categories of predictions, namely the ones that predict $\Delta d/d$ stays negative (LO and NLO analyses of polarized DIS data: GRSV, LSS, AAC, GS, statistical model, and a quark-hadron duality scenario) and the ones predicting $\Delta d/d \to 1$ when $x \to 1$ (leading order pQCD and a quark-hadron duality scenario).

readout as detector for the low-energy spectator proton in the reaction $en(p_s) \to ep_sX$. Measurement of the spectator proton for momenta as low as 70 MeV/c and at large angles allows to minimize poorly known nuclear corrections at large x. The techniques can be used with `CLAS12` at 12 GeV to accurately determine the ratio $d(x)/u(x)$ to much larger x values. Figure 6 shows the projected data for $F_2^n(x)/F_2^p(x)$ and $d(x)/u(x)$. A dramatic improvement can be achieved at large x.

4.2 Spin structure functions and parton distributions

JLab PAC30 also approved E12-06-109 [23] which will, in particular, study polarized parton distributions at large x. Using standard detection equipment, a redesigned polarized target adapted to `CLAS12` and 30 (50) days of running on a longitudinally polarized NH_3 (ND_3) target, high precision measurements can be achieved as shown in Fig. 7. These data will disentangle models in the large-x region. While the results shown in Fig. 7 are with a $W > 2$ GeV constraint, hadron-parton duality studies will tell us by how much this constraint can be relaxed, possibly increasing the x range up to 0.9. The expected accuracy for $(\Delta d + \Delta\bar{d})/(d + \bar{d})$ is shown in Fig. 8.

4.3 Global Fit of Polarized Parton Distributions

The large window opened by the 12 GeV upgrade over the DIS domain will permit constraints of global fits of

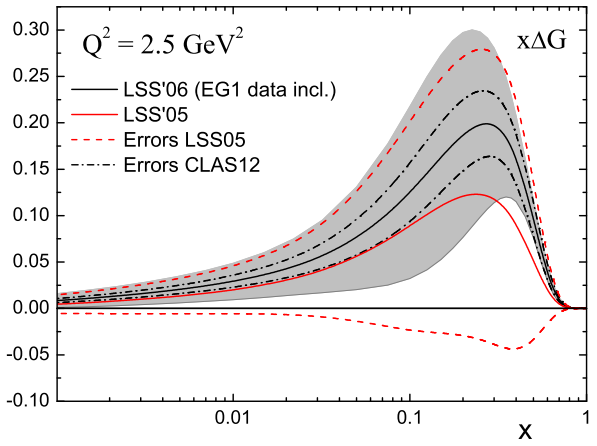

Fig. 9. Expected uncertainties for $x\Delta G$. The black solid curve shows the central value of the present analysis that includes CLAS EG1 data. The dashed-dotted lines give the error band when the expected `CLAS12` data are included in the LSS QCD analysis.

the parton distributions. JLab data at lower energies had already unique impact at large x. The improvement from the 12-GeV upgrade is also significant at low and moderate x, noticeably for the polarized gluon distribution ΔG. To demonstrate the precision achievable with the expected `CLAS12` data, we have plotted in Fig. 9 an analysis of the impact on NLO analyses of the polarized gluon distribution [24]. A dramatic improvement can be achieved with the expected data from the `CLAS12` proposal E12-06-109 [23]. We emphasize that the data will not only reduce the error band on ΔG, but will likely allow a more detailed modeling of its x-dependence. Significant improvements are expected for the quark distributions as well.

4.4 Moments of spin structure functions.

Moments of structure functions provide powerful insight into nucleon structure. Inclusive data at JLab have permitted evaluation of the moments at low and intermediate Q^2 [25,26,27]. With a maximum beam energy of 6 GeV, however, the measured strength of the moments becomes rather limited for Q^2 greater than a few GeV^2. The 12-GeV upgrade removes this problem and allows for measurements to higher Q^2.

Moments of structure functions can be related to the nucleon static properties by sum rules. At large Q^2 the Bjorken sum rule relates $\int g_1^{p-n} dx$ to the nucleon axial charge [31]. Figure 10 shows the expected precision on Γ_1^p. Published results and preliminary results from EG1b are also displayed for comparison. The hatched blue band corresponds to the systematic uncertainty on the EG1b data points. The red band indicates the estimated systematic uncertainty from `CLAS12`. The systematic uncertainties for EG1 and `CLAS12` include the estimated uncertainty

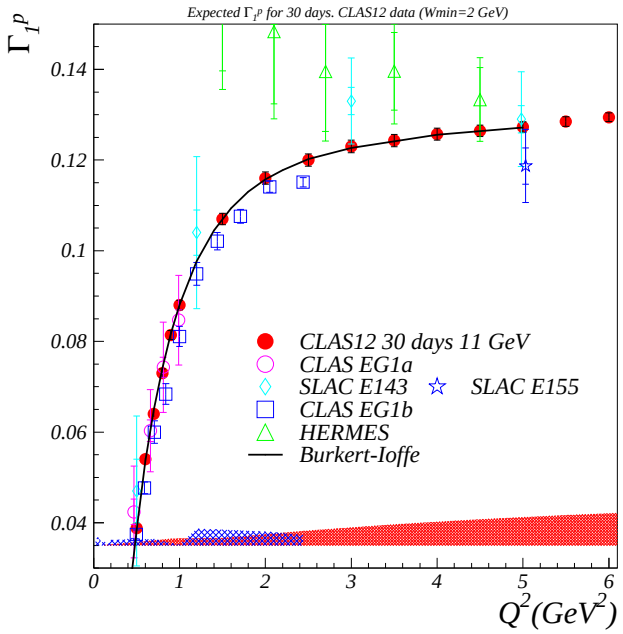

Fig. 10. Left plot: expected precision on Γ_1^p for CLAS12 and 30 days of running. CLAS EG1a [25,26] data and preliminary results from EG1b are shown for comparison. The data and systematic uncertainties include estimates of the unmeasured DIS contribution. HERMES [28] data, and E143 [29] and E155 data [30] from SLAC are also shown (including DIS contribution estimates). The model is from Burkert and Ioffe [32,33].

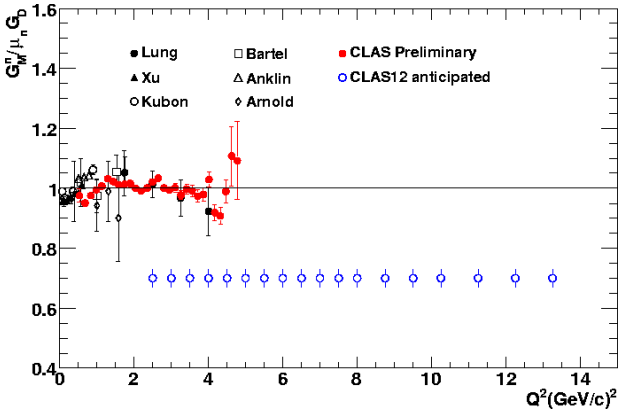

Fig. 11. The magnetic form factor for the neutron. The existing data, and projected uncertainties at 12 GeV with CLAS12 (blue open circles).

on the unmeasured DIS part estimated using the model from Bianchi and Thomas [34]. As can be seen, moments can be measured up to Q^2=6 GeV^2 with a statistical accuracy improved several fold over that of the existing world data.

Finally, moments in the low ($\simeq$ 0.5 GeV^2) to moderate ($\simeq$4 GeV^2) Q^2 range enable us to extract higher-twist parameters, which represent correlations between quarks in the nucleon. This extraction can be done by studying the Q^2 evolution of first moments [35,36]. Higher twists have been consistently found to have, overall, a surprisingly smaller effect than expected. Going to lower Q^2 enhances the higher-twist effects but makes it harder to disentangle a high twist from the yet higher ones. Furthermore, the uncertainty on α_s becomes prohibitive at low Q^2. Hence, higher twists turn out to be hard to measure, even at the present JLab energies. Adding higher Q^2 to the present JLab data set removes the issues of disentangling higher twists from each other and of the α_s uncertainty. The smallness of higher twists, however, requires statistically precise measurements with small point-to-point correlated systematic uncertainties. Such precision at moderate Q^2 has not been achieved by the experiments done at high energy accelerators, while JLab at 12 GeV presents the opportunity to reach it considering the expected statistical and systematic uncertainties of E12-06-109. The total point-to-point uncorrelated uncertainty on the twist-4 term for the Bjorken sum, f_2^{p-n}, decreases by a factor of 5.6 compared to results obtained in Ref. [37].

5 Nucleon form factors and resonance transitions at short distances

The most basic observables that reflect the composite nature of the nucleon are its electromagnetive form factors. Historically the first direct indication that the nucleon is not elementary came from measurements of these quantities in elastic *ep* scattering [38]. The electric and magnetic form factors characterize the distributions of charge and magnetization in the nucleon as a function of spatial resolving power. The transition form factors reveal the nature of the excited states of the nucleon. Further, these quantities can be described and related to other observables through the GPDs.

Measurements of the elastic form factors will remain an important aspect of the physics program at 12 GeV, and will be part of the program in other experimental Halls at JLab. The magnetic form factor of the neutron, as well as the transition form factors for several prominent resonances require special experimental setups for which CLAS12 is suited best. Figure 11 shows the current data as well as the extension in Q^2 projected for the 12 GeV program with CLAS12.

Nucleon ground and excited states represent different eigenstates of the Hamiltonian, therefore to understand the interactions underlying nucleon formation from fundamental constituents, the structure of both the ground state and the excited states must be studied. The current N^* program at Jlab has already generated results for the transition form factors at Q^2 up to 6 GeV^2 for the $\Delta(1232)$ [39, 40,41], and up to 4 GeV^2 for the $N(1535)S_{11}$ [42,43,44]. The most recent results [45,46] on the transition form factors for the Roper resonance $N(1440)P_{11}$ for Q^2 up to 4.5 GeV^2, have demonstrated the sensitivity to the degrees of freedom that are effective in the excitation of particular states. The JLab energy upgrade will allow us to probe

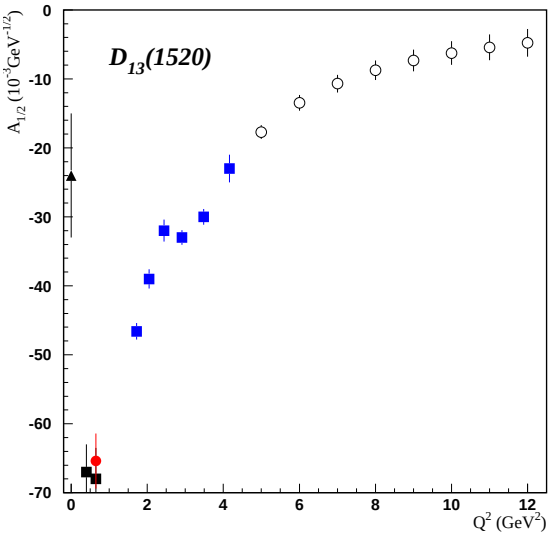

Fig. 12. The transverse photocoupling amplitude $A_{1/2}$ for the $N(1520)D_{13}$ resonance. The blue full squares are preliminary data from CLAS. The open circles represent projected results with CLAS12 at 12 GeV.

resonance excitations at much higher Q^2, where the relevance of elementary quarks in the resonance formation may become evident through the approach to asymptotic scaling. Figure 12 shows projected Q^2 dependence of the $A_{1/2}$ transition amplitude for the $N(1520)D_{13}$ resonance obtained from single pion production. Higher mass resonances may be efficiently measured in double-pion processes [47,48] such as $ep \rightarrow ep\pi^+\pi^-$.

6 Conclusions

The JLab energy upgrade and the planned new experimental equipment are well matched to an exciting scientific program aimed at studies of the complex nucleon structure in terms of the newly discovered longitudinal and transverse momentum dependent parton distribution functions, the GPDs and TMDs. They provide fundamentally new insights in the complex multi-dimensional structure of the nucleon. In addition, the high precision afforded by the high luminosity and the large acceptance detectors, and the development of novel techniques to measure scattering off nearly free neutrons, will allow the exploration of phase space domains with extreme conditions that could not be studied before.

Acknowledgment

I am grateful to members of the CLAS collaboration who contributed to the development of the exciting physics program for the JLab upgrade to 12 GeV, and the CLAS12 detector. Much of the material in this report is taken from the CLAS12 Technical Design Report Version 3, October 2007 [49].

This work was supported in part by the U.S. Department of Energy and the National Science Foundation, the French Commisariat á l'Energie Atomique, the Italian Instituto Nazionale di Fisica Nucleare, the Korea Research Foundation, and a research grant of the Russian Federation. The Jefferson Science Associates, LLC, operates Jefferson Lab under contract DE-AC05-060R23177.

References

1. X. Ji, Phys. Rev. D**55**, 7114, 1997.
2. X. Ji, Phys. Rev. Lett.**8**, 610, 1997.
3. A. Radyushkin, Phys. Lett. B**380**, 417, 1996.
4. A. Radyushkin, Phys. Rev. D**56**, 5524, 19
5. B. Mecking et al., Nucl. Inst. Meth. A**503**,513, 2003.
6. M. Vanderhaeghen, P. Guichon, M. Guidal, Phys. Rev. D**60**, 094017, 1999.
7. JLAB experiment E12-06-119, F. Sabatie *et al.*
8. A. Belitsky, D. Mueller, A. Kirchner, Nucl. Phys. B**629**, 323, 2002.
9. M. Burkardt, Int. J. Mod. Phys. A**18**, 173, 2003.
10. A.V. Belitsky, X. Ji, F. Yuan, Phys. Rev. D**69**, 074014, 2004.
11. K. Goeke *et al.*, Phys. Rev. D**75**, 094021, 2007.
12. S. Stepanyan *et al.*, Phys. Rev. Lett.**87**, 182002, 2001.
13. F.X. Girod, *et al.*, arXiv:0711.4805 [hep-ph], subm. to Phys. Rev. Lett..
14. C. Munoz-Camacho *et al.*, Phys. Rev. Lett.**97**, 262002, 2006.
15. S. Chen *et al.*, Phys. Rev. Lett.**97**, 072002, 2006.
16. X. Ji, J.-P. Ma, F. Yuan, Nucl. Phys. B**652**, 383, 2003.
17. JLab experiment E12-07-107, H. Avakian *et al.*.
18. JLab Experiment E03-12, H. Fenker, C. Keppel, S. Kuhn, W. Melnitchouk, *et al.*
19. JLAB Experiment E12-06-113, S. Bueltman *et al.*
20. X. Zheng *et al.*, Phys. Rev. C70, 065207, 2004.
21. V. Dharmawardane, *et al.*, Phys. Lett. B**641**, 11, 2006.
22. P. Bosted *et al.*, Phys. Rev. C**75**, 035203, 2007.
23. JLab experiment E12-06-109, S. Kuhn *et al.*
24. E. Leader, S. Sidorov, D. Stamenov, Phys. Rev. D**75**, 074027, 2007.
25. R. Fatemi *et al.*, Phys. Rev. Lett.**91**, 222002, 2003.
26. J. Yun *et al.*, Phys. Rev. C**67**, 055204, 2003.
27. M. Amarian et al., Phys. Rev. Lett. **92**, 022301, 2004.
28. A. Airapetian et al.,Eur. Phys. J.C**26**, 527, 2003.
29. K. Abe *et al.*, Phys. Rev. D**58**, 112003, 1998.
30. P.L. Anthony *et al.*, Phys. Lett. B**493**, 19, 2000.
31. J.D. Bjorken, Phys. Rev. **148**, 1467, 1966.
32. V.D. Burkert, B.L. Ioffe, Phys. Lett. B**296**, 223, 1992.
33. V.D. Burkert, B.L. Ioffe, J. Exp. Theor. Phys.**78** , 619, 1994.
34. E. Thomas, N. Bianchi, Nucl. Phys. Proc.Suppl.**82**, 26, 2000.
35. M. Osipenko *et al.*, Phys. Rev. D**71**, 054007, 2005.
36. J.P. Chen, A. Deur, Z.-E. Meziani, Mod. Phys. Lett. A**20**, 2745, 2005.
37. A. Deur, *et al.*, Phys. Rev. Lett.**93**, 212001, 2004.
38. R. Hofstadter and R.W. Allister, Phys. Rev. **98**, 183, 1955.
39. V. Frolov *et al.*, Phys. Rev. Lett.**82**, 45,1999.
40. K. Joo, *et al.*, Phys.Rev. Lett. **88**, 122001, 2002.
41. M. Ungaro *et al.*, Phys. Rev. Lett.**97**, 112003, 2006.
42. C. Armstrong *et al.*, Phys. Rev. D**60**, 052004, 1999.
43. R. Thompson *et al.*, Phys. Rev. Lett.**86**, 1702, 2001.
44. H. Denizli *et al.*, Phys. Rev. C**76**, 015204, 2007.
45. K. Park *et al.*, arXiv:0709.1946, accepted by Phys. Rev. C.
46. I. Aznauryan and V.D. Burkert, arXiv:0711.1120 [nucl-th].
47. M. Ripani *et al.*, Phys. Rev. Lett.**91**, 022002, 2003.
48. V. Mokeev, invited talk presented at this conference.
49. The complete document may be obtained from the author.